Polymer 235 (2021) 124266

Contents lists available at ScienceDirect

Polymer

journal homepage: www.elsevier.com/locate/polymer

Multi-stimuli responsive fluorescence chemosensor based on diketopyrrolopyrrole-based conjugated polyfluorene

Mohamed Gamal Mohamed [a,b], Yu-Shan Chou [c], Po-Chih Yang [c,*], Shiao-Wei Kuo [a,d,**]

[a] Department of Materials and Optoelectronic Science, Center of Crystal Research, National Sun Yat- Sen University, Kaohsiung, 804, Taiwan
[b] Chemistry Department, Faculty of Science, Assiut University, Assiut, 71516, Egypt
[c] Department of Chemical Engineering and Materials Science, Yuan Ze University, Taoyuan, 32003, Taiwan
[d] Department of Medicinal and Applied Chemistry, Kaohsiung Medical University, Kaohsiung, 807, Taiwan

ARTICLE INFO

Keywords:
Diketopyrrolopyrrole
Suzuki coupling polymerization
Chemosensor
Conjugated polyfluorene

ABSTRACT

Herein, we successfully prepared a conjugated polyfluorene (PFDPP) containing two different kinds of diketopyrrolopyrrole (DPP) derivatives (M1 and M2) through Suzuki polymerization. The chemical sensing and optical properties of PFDPP were investigated and discussed in detail in the presence of different cations and anions. The Photoluminescence (PL) titrations results demonstrated that the Stern-Volmer constants (K_{sv}) and the limit of detection (LOD) of PFDPP were 2.30×10^5 M^{-1} and 1.31×10^{-6} M for Fe^{3+} and 1.05×10^5 M^{-1} and 1.81×10^{-6} M for F^-. In addition, we observed that PFDPP solution showed complete emission quenching when pH increased from 11 to 13 owing to the protonation for DPP structures. Therefore, we expect the PFDPP material could be used as a good candidate for chemosensory and other environmental applications.

1. Introduction

Because of amazing potential applications in chemical and biochemical sensors, fluorescent conjugated polymer-derived fluorescent chemosensors it has aroused great interest for pH measurement, various metal ions, and analytes detection by changing in fluorescence intensity and color [1–18]. π-Conjugated polyfluorenes (PFs) are promising candidates for various optoelectronic applications, i.e., field-effect transistors, polymer solar cells, electrochromic devices, and fluorescent chemosensors, owing to their facile postmodification of the fluorene moiety at the 9,9-positions and high PL quantum yield [19–21]. To date, a series of PFs bearing sulfonic (SO_3H), imidazole, phosphonate, and ammonium at the 9,9-dialkyl chains of the fluorene ring have been synthesized to detect metal ions [22–24].

Due to the highly planar conjugated bicyclic structure of the diketopyrrolopyrrole (2,5-dihydropyrrolo[4,3-c]pyrrolo-1,4-dione, DPP) unit and the presence of carbonyl groups in its structure, which leads to hydrogen bonding formation and strong π-π molecular interactions [25–36]. However, the presence of various strong interactions such as π-π intermolecular interactions and H-bonding in the DPP-based materials leads to insoluble these materials in common organic solvents [37–39]. To enhance and improve the solubility efficiently, reduce the interchain interaction, and inhibited polymer chain alignment for materials based on DDP units by adding some long flexible chain groups such as alkyl or ethylene glycol group in the DPP moiety (the lactam N atoms position) [40].

DPPs are widely used as fluorescent dye because of their facile preparation, high quantum yield, excellent thermal stability, photochemical properties, and intense color [41]. This class of compounds incorporating π-linker (e.g., thiophene or phenyl) at 3,6-positions of the DPP unit have been understood as a regulatory unit for improving the performance of fluorescent chemosensors and organic semiconductors [42]. Furthermore, the DPP based on conjugated polymers has been much attracted and applied in various potential applications such as field-effect transistor materials, chemical sensing for cations and anions, biological imaging; fluorescence tags, and organic photovoltaic and field-effect transistor materials [43–48]. Qu et al. [49] successfully synthesized DPP materials and these materials exhibited a red emission color toward fluoride ion with detection limit values of 2.46 and 4.20 μM in acetonitrile and acetone, respectively.

In this work, we prepared a DPP-based polymer (PFDPP) containing two different kinds of DPP monomers (M1 and M2) with pyridinyl unit

* Corresponding author. Department of Chemical Engineering and Materials Science, Yuan Ze University, Taoyuan, 32003, Taiwan.
** Corresponding author. Department of Materials and Optoelectronic Science, Center of Crystal Research, National Sun Yat- Sen University, Kaohsiung, 804, Taiwan.
E-mail addresses: pcyang@saturn.yzu.edu.tw (P.-C. Yang), kuosw@faculty.nsysu.edu.tw (S.-W. Kuo).

https://doi.org/10.1016/j.polymer.2021.124266
Received 15 September 2021; Received in revised form 4 October 2021; Accepted 9 October 2021
Available online 11 October 2021
0032-3861/

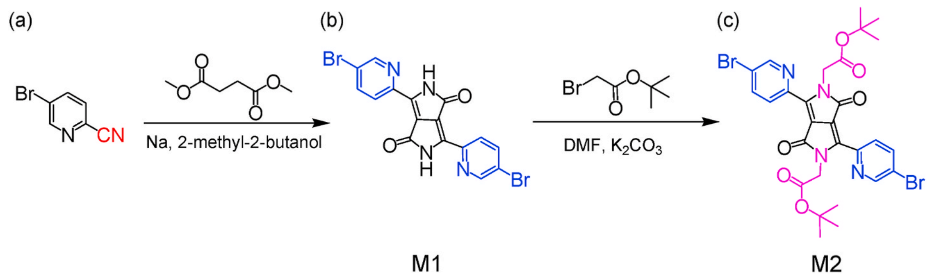

Scheme 1. Synthesis of M1 and M2.

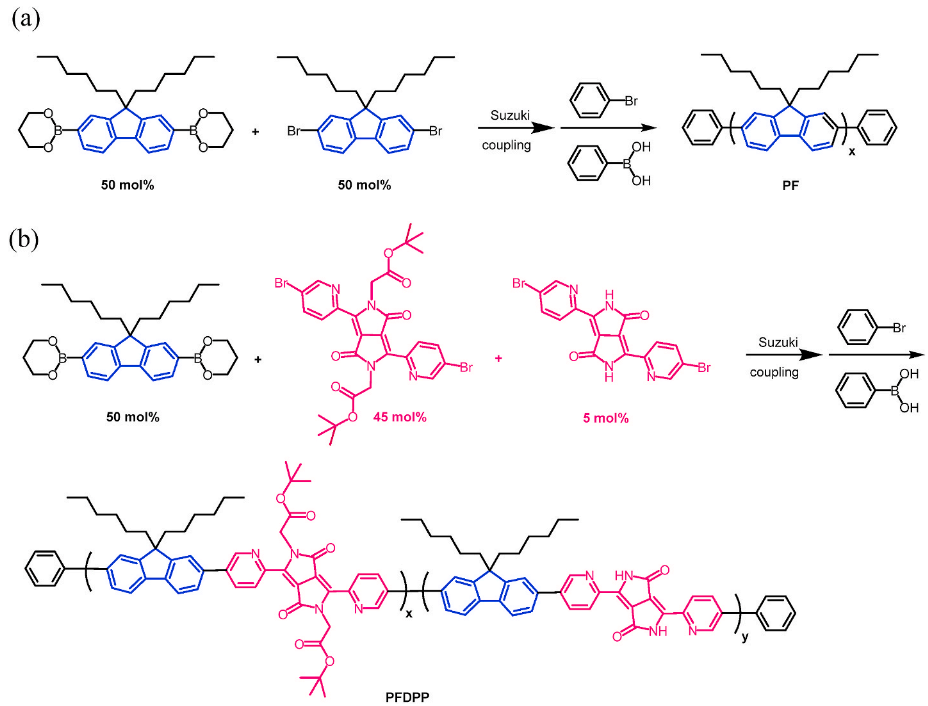

Scheme 2. Synthetic routes of (a) PF and (b) PFDPP.

as π-linker to amplify the fluorescent signal and recognized performance in cation ion addition process, owing to the large electronegativity and lone pair of a nitrogen atom. M2 is composed of *tert*-butyl propionate units in the DPP lactam N atoms positions to improve the solubility. In contrast, M1 still contains only the DPP lactam N atoms to recognize with fluorine ions. To the best of our knowledge, only a few reports for preparation of the DPP derivatives incorporating pyridinyl π-linker have been done. In this present work, we found that PFDPP material displays the highly dual selective response to Fe^{3+} and F^-, with the K_{sv} of 2.3 × 10^5 M^{-1} and 1.05 × 10^5 M^{-1}, respectively. In addition, when pH values of PFDPP solution increase from 7 to 10, the emission color solutions change from yellow to pale green; however, when the pH value increased to 13, the solution color changed to blue. Our results suggest that PFDPP can be used as multi-stimuli responsive fluorescence chemosensors for cations and anions.

2. Experimental

2.1. Materials

5-Bromo-2-cyanopyridine (98%), dimethyl succinate (98%), 2-methyl-2-butanol (98%), *tert*-butyl bromoacetate (98%), benzeneboronic acid (98%), bromobenzene (99%), iron(II), magnesium, copper(II), zinc(II) chlorides (99%), lead(II) nitrate, silver nitrate, aluminium nitrate Aliquat 336 were ordered from Alfa Aesar. 9,9-Dihexyl-2,7-dibromofluorene (98%), 9,9-dihexylfluorene-2,7-diboronic acid bis (1,3-propanediol) ester (DF) (97%), sodium cyanide (95%), and potassium bromide (99%) were purchased from Sigma-Aldrich. Iron(III) chloride (95%), tetrakis(triphenylphosphine) palladium(0) (99%), mercury(II) chloride (99.5%), tetra-*n*-butylammonium fluoride, sodium nitrate, and sodium bisulfate (92%) were ordered from Across. Potassium chloride (99%), potassium carbonate (K_2CO_3, 99.5%), nickel(II) chloride (96%), sodium chloride (99.5%), Potassium iodide (KI), sodium nitrite (98.5%) and calcium chloride (95%) were ordered from SHOWA. lithium chloride (99%) was ordered from MERCK. Barium chloride was purchased from Shimakyu's pure chemicals. Synthetic routes for the DPP-functionalized monomers (3,6-bis(5-bromopyridin-2-yl)-2,5-dihydropyrrolo[3,4-*c*]pyrrole-1,4-dione (M1) and di-*tert*-butyl 2,2'-(3,6-bis (5-bromopyridin-2-yl)-1,4-di-oxopyrrolo[3,4-*c*] pyrrole-2,5(2*H*,5H)-diyl) diacetate (M2)) are shown in Scheme 1 and more details in the supplementary information (SI). The synthetic route for the target conjugated polymer (PFDPP) or poly(9,9-dihexylfluorene) (PF) are shown in Scheme 2.

2.2. Synthesis of PFDPP

M1 (0.0134 g, 0.03 mmol), M2 (0.1826 g, 0.27 mmol), DF (0.15 g, 0.3 mmol), and $Pd(PPh_3)_4$ (0.0173 g, 0.015 mmol) were dissolved in dry

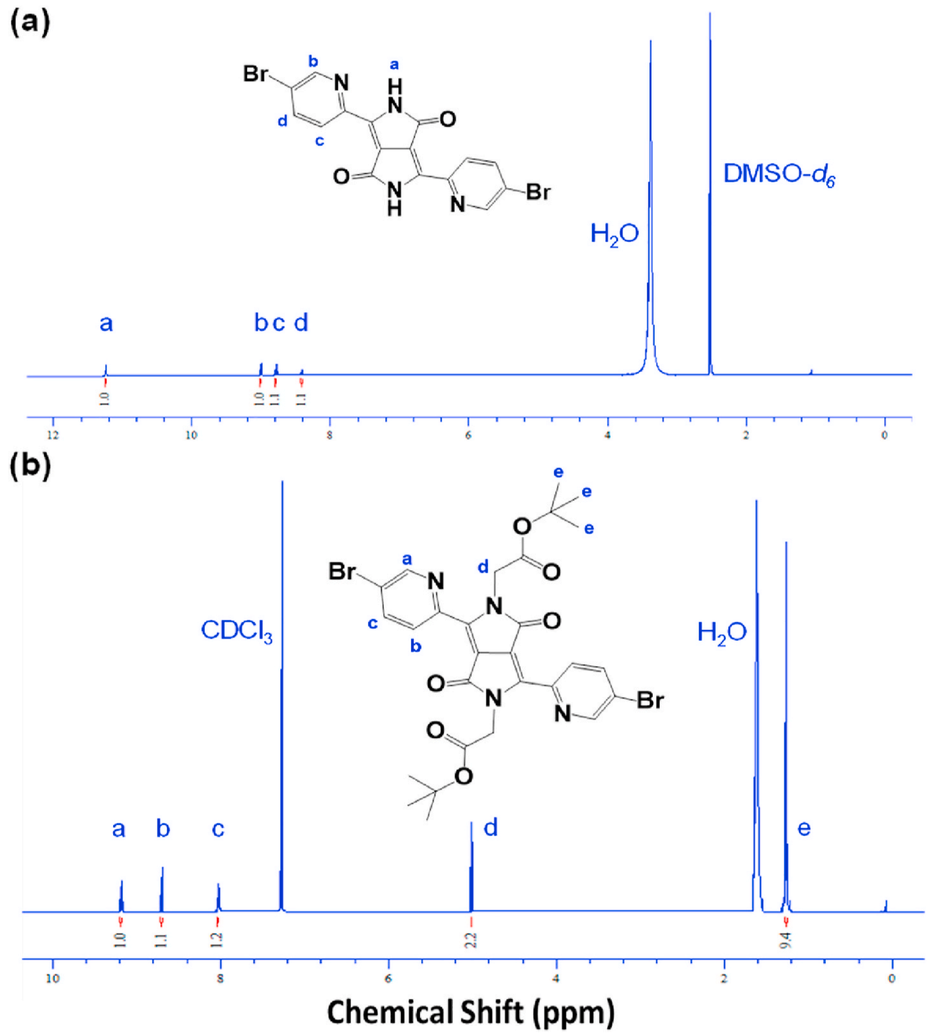

Fig. 1. ^{1}H NMR analyses of (a) M1 and (b) M2.

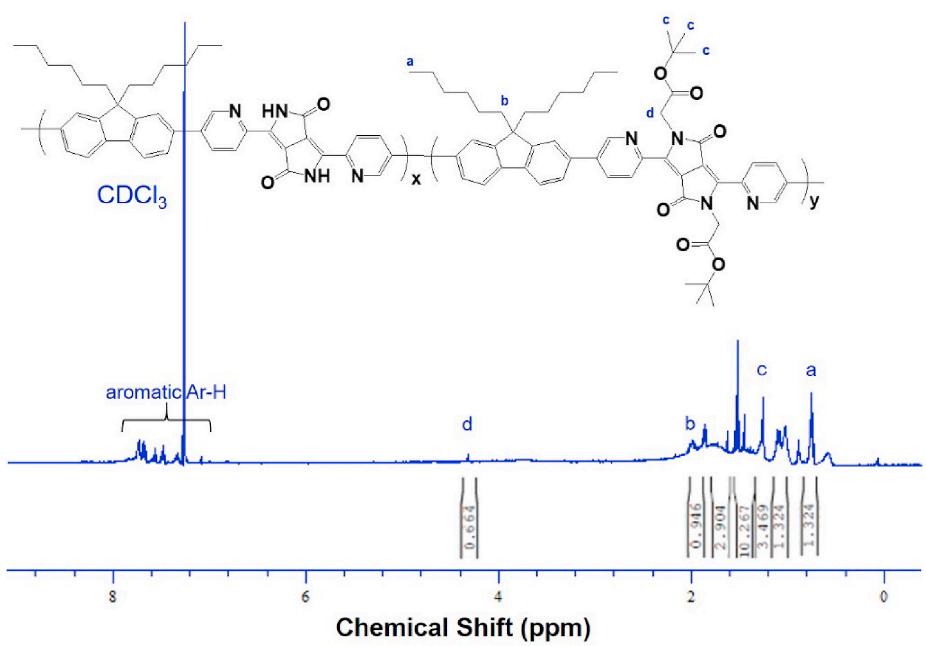

Fig. 2. ^{1}H NMR spectrum of PFDPP.

Table 1
Molecular weights and thermal properties of polymers.

Polymer	Yield (%)	M_w[a] (× 10^4)	PDI[a]	T_g (°C)[b]	T_d (°C)	DP (*x*:*y*)[d]
PF	40.2	2.18	2.01	153.3	414.7	31:0
PFDPP	66.7	0.74	1.74	—[c]	185.0	4:1

[a] M_w and PDI of polymer were determined by GPC.
[b] T_g by DSC under N_2 at a heating rate of 10 °C/min.
[c] Not observed.
[d] Degrees of polymerization (DP) of PF and PFDPP was calculated by GPC and ^{1}H NMR spectra, respectively.

DMF (5 mL) and then, 4 mL of K_2CO_3 solution (2.0 M) was added. After the solution was heated at 80 °C for 24 h. Phenylboronic acid (12.2 mg, 0.2 mmol) and bromobenzene (15.7 mg, 0.2 mmol) were both added. After refluxing for 6 h, the solution was poured into the excess of CH_3OH solution to afford PFDPP (Yield: 66.7%). ^{1}H NMR ($CDCl_3$, 400 MHz, δ, ppm) = 0.75–0.76 (CH_3), 1.06–1.10 (CH_2), 1.25 (CH_3), 1.85 (CH_2), 1.97–2.03 (CH_2), 4.32 (NCH_2), 7.12–7.14 (Ar–H), 7.46–7.49 (Ar–H), 7.55–7.57 (Ar–H), 7.65–7.84 (Ar–H).

2.3. Fluorescent titration with various metal ions

Various nitrate and chloride salts solution with a concentration of 1.0×10^{-3} M was prepared in DI water and the fluorescent titration was measured by adding polymer solution to each bottle of salt solution. The stabilization of PFDPP-anion complexes in THF as a solvent was tested in the presence of NO_3^-, F^-, CN^-, HSO_4^-, Br^-, I^-, NO_2^-, HSO_4^-, Cl^-, SCN^-, and PO_4^{3-}. The concentration of the PF and PFDPP during the PL titrations was 1×10^{-5} M.

3. Results and discussion

3.1. Synthesis of the DPP-functionalized monomers, PF and PFDPP

Scheme 1 presented the method for the synthesis of two monomers based on the DPP unit (M1 and M2). Firstly, M1 was prepared by using a literature method with a slight modification method [50]. The solubility of monomer (M1) was improved by the reaction of M1 with *tert*-butyl bromoacetate, leading to the formation of M2. The resulting M2 was dissolved in toluene, chloroform, and THF. Fig. 1 shows ^{1}H NMR spectra of the M1 and M2; respectively. As shown in Fig. 1(a), the signals appeared at 11.24 (H_a), and 9.00 (H_b) due to protons of the lactam NH and pyridinyl unit, respectively. The ^{1}H NMR spectrum of M2 (Fig. 1(b)) showed the peaks centered at 9.16 (H_a) and 8.02–8.69 ppm (H_b and H_c), which was ascribed to the pyridinyl moiety and doublet aromatic proton; respectively. We found that the lactam NH proton signal disappeared, whereas the additional singlet proton signals in the ^{1}H NMR spectrum of M_2 appeared at 4.99 (H_d) and 1.25 ppm (H_e) due to the methylene group adjacent to the lactam N atoms and the methyl groups. This indicates that M2 monomer was successfully synthesized from M1.

Table 2
Optical properties of conjugated polymers.

Polymer	UV–vis λ_{max} sol'n (nm)	UV–vis λ_{max} film (nm)	PL λ_{max} sol'n (nm)	PL λ_{max} film (nm)	Stokes Shift[a]	Φ_{PL}[b]
PF	380	383	416, 438, 475s	424, 444, 483s	41	1.00
PFDPP	489, 521	492, 520	547, 578	544, 581s	52	0.75

[a] Stokes shift = $PL_{(film)}$/nm – $UV_{(film)}$/nm.
[b] The quantum yield value measured by using PF as a standard.

PF and PFDPP polymers were successfully prepared by using a simple Suzuki coupling reaction of 9,9-dihexyl-2,7-dibromofluorene, DF with bromobenzene and phenylboronic acid for PF synthesis (Scheme 2(a)), and Suzuki coupling reaction of M1, M2, and DF with bromobenzene and phenylboronic acid for PFDPP preparation as displayed in Scheme 2 (b). The molar ratio feeding of M1 during polymerization was controlled as 5 mol% because of the poor solubility in DMF. Fig. 2 presents the ^{1}H NMR spectrum of PFDPP in $CDCl_3$, recorded at room temperature. The ^{1}H NMR spectrum of PFDPP exhibited signals at 7.12–7.84 ppm, which

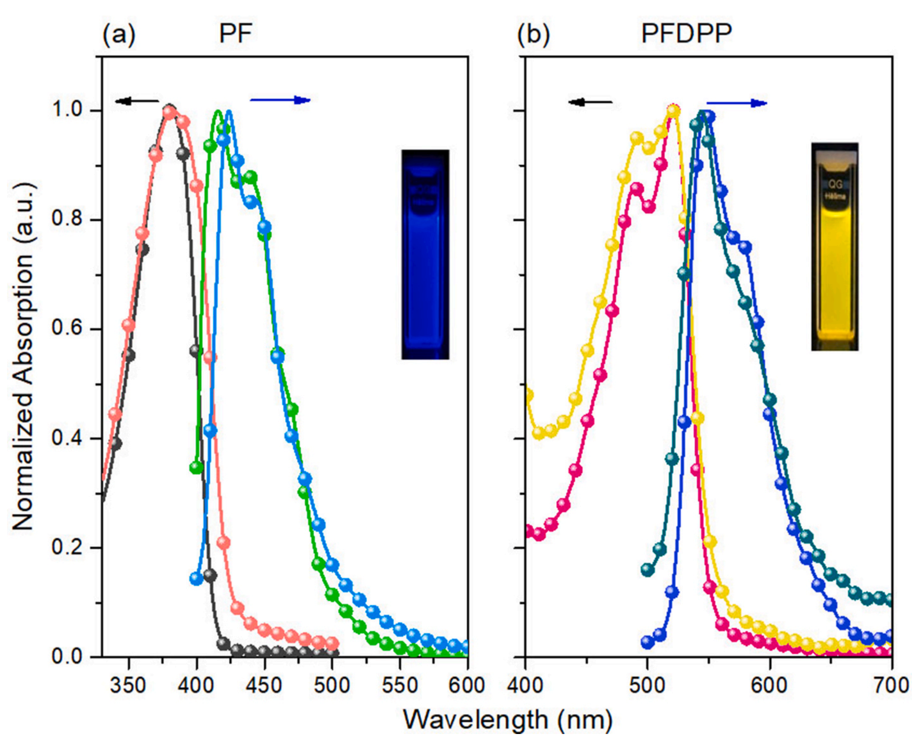

Fig. 3. Normalized absorption and photoluminescence spectra of (a) PF and (b) PFDPP in THF solution (solid line) and in thin film (dotted line).

Table 3
Optical and electrochemical properties of polymers.

No.	UV–vis λ_{onset}	$E_{ox\ (onset)}$ (V)	$E_{red\ (onset)}$ (V)	E_{HOMO}[a] (eV)	E_{LUMO}[b] (eV)	$E_{g\ (opt)}$[c] (eV)	$E_{g\ (el)}$[d] (eV)	E_g^{gau}[e] (eV)
PF	423	0.85	—[f]	−5.65	−2.72	2.93	–	3.72
PFDPP	554	0.36	−1.34	−5.16	−3.46	2.24	1.70	2.38

[a] $E_{HOMO} = -(E_{ox} + 4.8)$ eV.
[b] $E_{LUMO} = E_{HOMO} + E_{g\ (opt)}$ for PF and $E_{LUMO} = -(E_{red} + 4.8)$ for PFDPP.
[c] $E_{g\ (opt)} = 1240.8/\lambda_{onset}$.
[d] $E_{g\ (el)} = |E_{HOMO} - E_{LUMO}|$.
[e] Band gaps estimated from Gaussian 09 data.
[f] Not observed.

were assigned to the presence of DPP and fluorene moieties. The methylene singlet proton signals labeled H_d of M2 appeared at 4.32 ppm, whereas the methyl protons (H_c) of the *tert*-butyl units appeared at 1.25 ppm. Finally, the ^{1}H NMR spectrum of PFDPP had signals centered at 0.75–0.76 and 1.97–2.03 ppm assigned to the aliphatic protons (H_a and H_b). The other aliphatic methylene protons appeared at 1.06–1.85 ppm. The M_w, PDI index, and thermal properties of PF and PFDPP were summarized in Table 1.

3.2. Optical properties of the PF and PFDPP

Fig. 3 displays UV–vis and PL spectra of the PF and PFDPP in THF solution and their data are tabulated in Table 2. The PF solution had an absorption peak (Fig. 3(a)) centered at 380 nm due to π-π* transitions of aromatic units in the PF and PFDPP. In contrast, the absorption spectrum of PFDPP in THF solution (Fig. 3(b)) displayed red shifted at 489 nm and higher than PF by approximately 109 nm was assigned to the electron migration from fluorene (donor moiety) to the DPP unit (acceptor unit), because of the intramolecular charge transfer (ICT) interactions. As seen in Fig. 3, when both polymers were excited at 350 nm, the PF and PFDPP solution showed strong emission in the blue ($\lambda_{max} = 416$ nm) and yellow region ($\lambda_{max} = 547$ nm), respectively. The Φ_{PL} of PFDPP was 0.75 by using PF as reference ($\Phi_{PL} = 1.0$). The absorbance spectra of M1 and M2 monomers in THF are shown in Fig. S1(a). M1 and M2 monomers had an absorption band at 400–550 ($\lambda_{max} = 511$ nm) and 400–560 nm ($\lambda_{max} =$ 521 nm), respectively. However, the emission band of PF is from 400 to 525 nm ($\lambda_{em} = 416$ nm), which overlapped with the emission band of PF. This behavior was assigned to an energy transfer from fluorene groups towards the DPP units, resulting in Förster resonance energy transfer (FRET) phenomena and redshifts to higher wavelength (ca. $\lambda_{max} = 547$ nm for PFDPP). The schematic representation of FRET was presented in Fig. S1(b).

3.3. Electrochemical properties of the PF and PFDPP

The cyclic voltammogram of the PF and PFDPP in CH_2Cl_2 was performed with 100 mV s^{-1} as a scanning rate as shown in Fig. S2 and Table 3. As observed, the oxidation peak was 0.85 V for the PF, and this peak was due to the occurring p-doping process of the conjugated polymer chain. Whereas the CV curve of PFDPP had the onset oxidation peak centered at 0.36 V. The decreasing of oxidation value of PFDPP relative to PF may come from the delocalization charge process over the extended conjugated system between fluorene and DDP moieties. The estimated values of HOMO energy levels −5.65 and −5.16 eV for PF and PFDPP; respectively. The onset reduction peak of PFDPP was observed at −1.34 V. The LUMO energy level of PFDPP was about −3.46 eV according to the equation $E_{LUMO} = -(E_{red} + 4.8)$. The optical band gaps (E_g^{opt}) of PF and PFDPP were 2.93 and 2.24 eV, respectively. Therefore, we found that the LUMO energy levels values were −2.72 and −3.46 eV for PF and PFDPP; respectively. Furthermore, we examined the frontier

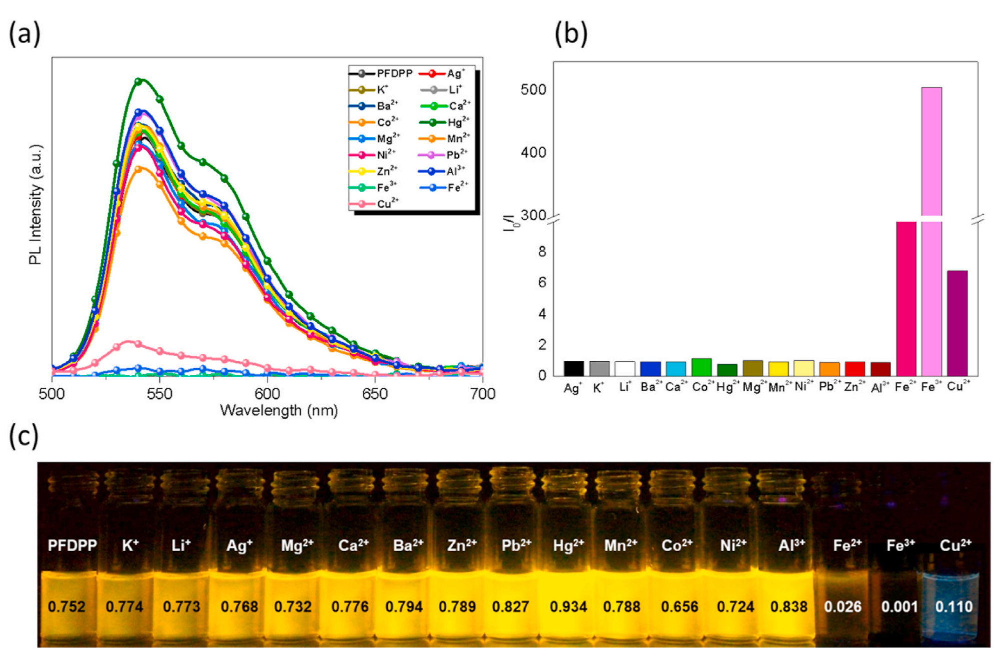

Fig. 4. (a) Photoluminescence spectra, (b) PL response profiles and (c) fluorescence colors of PFDPP (1.0×10^{-5} M) in the presence of various cation ions 5.5×10^{-5} M in water. Excitation wavelength: 350 nm. (For interpretation of the references to color in this figure legend, the reader is referred to the Web version of this article.)

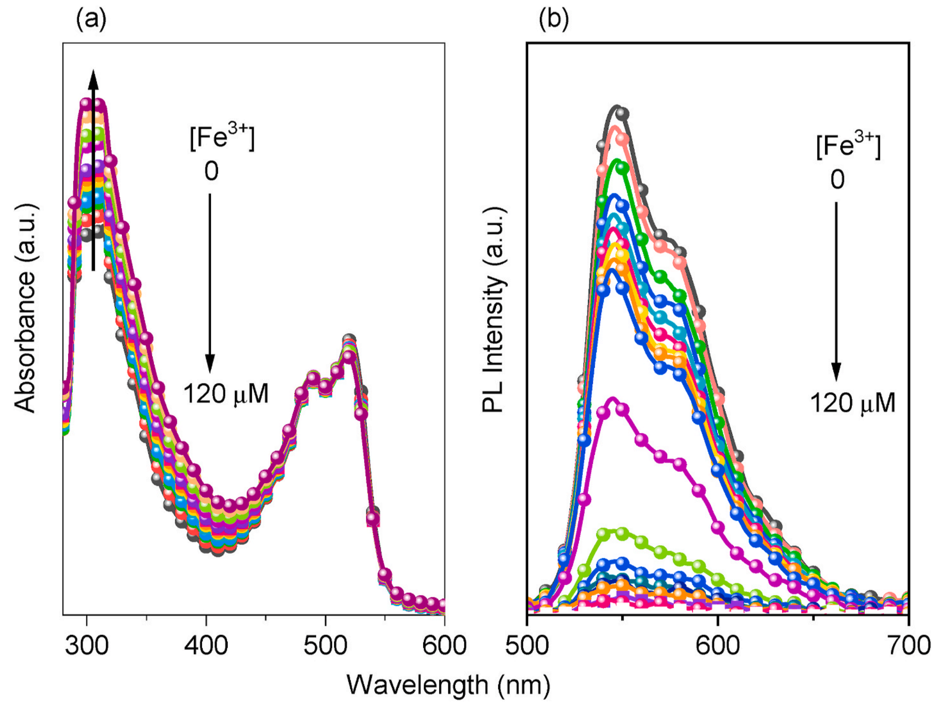

Fig. 5. (a) Absorption and (b) photoluminescence spectra of PFDPP in the presence of various concentrations of Fe^{3+}.

molecular orbitals and minimum-energy conformations of the model compounds of PF and PFDPP by using density functional theory (DFT) calculations as presented in Fig. S3. The DFT calculations showed that the HOMO and LUMO values were −5.16 and −1.44 eV, respectively for PF and they were −5.27 and −2.89 eV for PFDPP. In addition, the theoretical bandgap (E_g^{the}) value for PF and PFDPP was 3.72 and 2.38 eV, respectively and these values are different than the obtained E_g from CV data and UV–vis absorption analyses (*i.e.*, E_g^{opt} = 2.93 and 2.24 eV for PF and PFDPP). The results displayed that the model compound has a larger energy bandgap to the small repeating unit number and these data

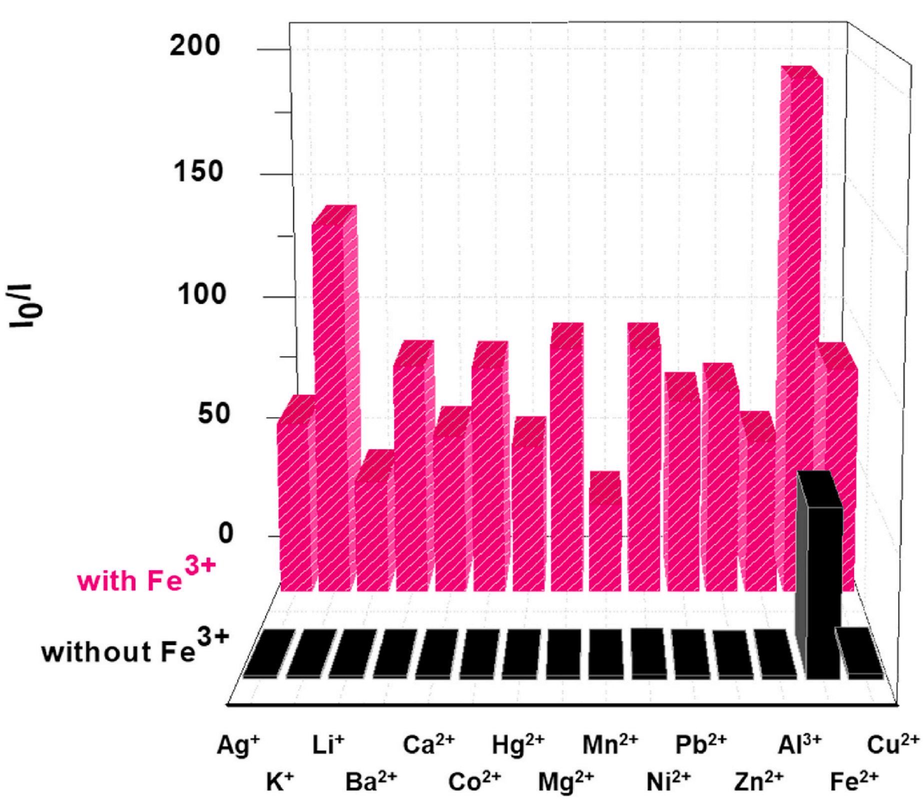

Fig. 6. Fluorescent quenching rate of PFDPP with different cations with or without Fe^{3+} ions in THF. The black bar represents the addition of the appropriate metal ion to a solution of the conjugated polymer. The red bar represents the subsequent addition of Fe^{3+} to the former solution. (For interpretation of the references to color in this figure legend, the reader is referred to the Web version of this article.)

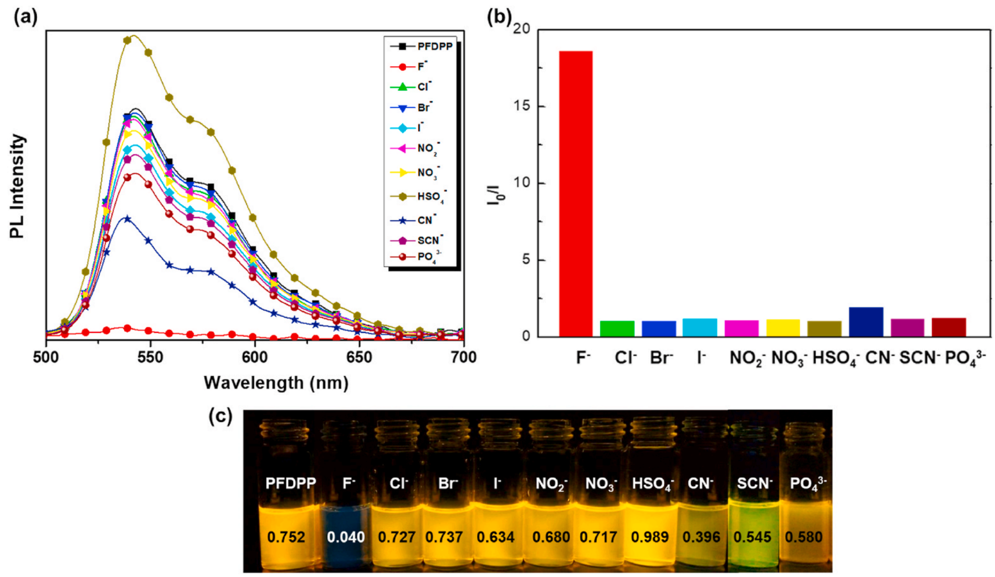

Fig. 7. (a) Photoluminescence analyses, (b) PL response profiles and (c) fluorescence colors of PFDPP in the presence of various anion ions (excitation: 350 nm). (For interpretation of the references to color in this figure legend, the reader is referred to the Web version of this article.)

confirmed that the incorporation of electron-acceptor groups like the DPP group into the polymer chain will reduce E_g values and effect on the LUMO level.

3.4. Cation sensing properties of the PFDPP

We expected that the presence of DDP as an electron acceptors group in the PFDPP polymer backbone will show different fluorescence colors in the presence of various metal cations and anions. Fig. 4(a) displays the changes in fluorescence color and intensity of PFDPP in the THF/H_2O solution upon the addition of various cations. The fluorescence intensity of PFDPP solution decreased significantly on the addition of Fe^{2+}, Fe^{3+}, or Cu^{2+} ions (Fig. 4(a)), indicating that energy transfer from the DPP chelating moiety in the conjugated polymer backbone to these metal cations and leading to quenching the emission of the PFDPP. The quenching mechanism of the polymer is attributed to the photoinduced energy transfer. These results suggest that the complexation between the N/O atoms of DPP core and N atom of pyridinyl segments and the positively charged cations led to the formation of a weak fluorescent complex. We observed that upon the addition of Fe^{3+} ions (1.0×10^{-4} M) into PFDPP solution, the fluorescence emission of PFDPP was quenched completely, indicating PFDPP has a great selectivity toward Fe^{3+}. We attributed the fluorescence quenching phenomena of PFDPP with Fe^{3+} ions for the strong coordination and effective binding between the DPP chelating groups and pyridinyl N atoms with Fe^{3+}. Fig. 4(b) shows the PL response profiles (*i.e.*, I_o/I) of PFDPP in the presence of

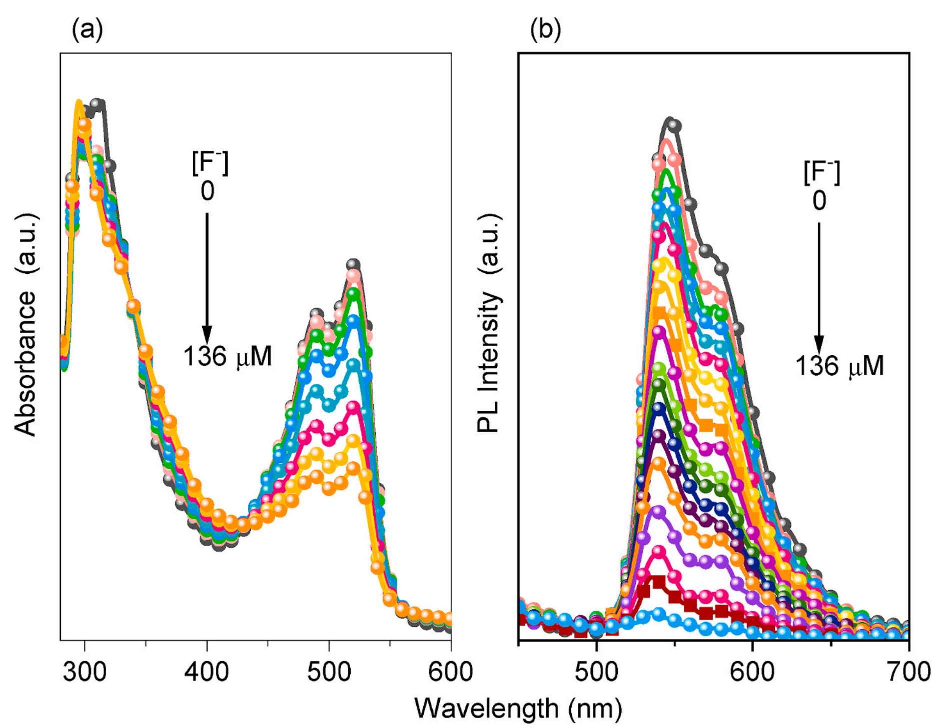

Fig. 8. (a) Absorption and (b) photoluminescence profiles of PFDPP in the presence of various concentrations of F^-.

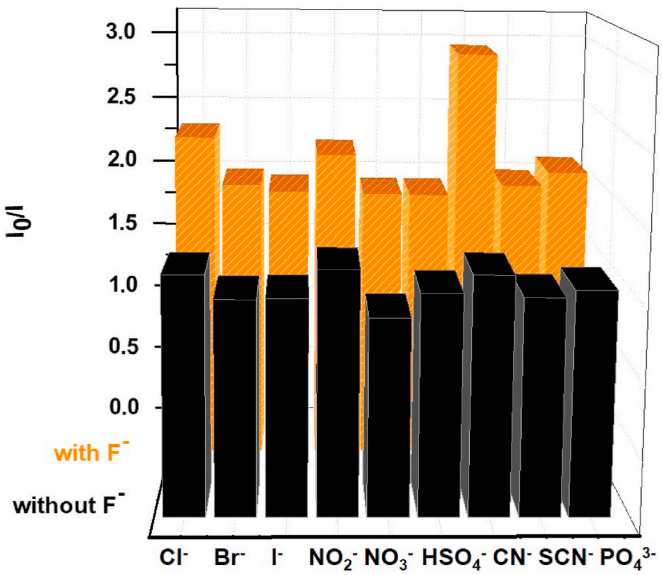

Fig. 9. Fluorescent quenching rate of PFDPP in the presence of different anions with or without F^- ions in THF. The black bar represents the addition of the appropriate anion ion to a solution of the conjugated polymer. The orange bar represents the subsequent addition of F^- to the former solution. (For interpretation of the references to color in this figure legend, the reader is referred to the Web version of this article.)

various metal cations. The changing emission colors of PFDPP upon addition metals cations were visible (Fig. 4(c)). As clearly seen, a marked fluorescence change from bright yellow to dark of PFDPP solution in the presence of Fe^{3+} in the THF-H_2O mixture. The Φ_{PL} value of PFDPP decreased from 0.75 to be 1.0×10^{-3} in the presence of Fe^{3+} ions.

Upon addition of Fe^{3+} and concentration increase, PFDPP had absorption spectra in the range of 290–450 nm with higher intensities [Fig. 5(a)], which resulted from the interaction between DPP chelating moiety and Fe^{3+}. Fig. 5(b) shows the fluorescence titration behavior response of PFDPP with Fe^{3+} in the THF. Based on PL data, with increasing concentrations of Fe^{3+}, the emission intensities peak of PFDPP at 547 nm gradually decreased. At low concentrations of Fe^{3+} cations below 2.0×10^{-5} M, the K_{sv} values of PFDPP were 2.30×10^5 M^{-1}. The detection limit for PFDPP toward Fe^{3+} was 1.31×10^{-6} M and this indicates that PFDPP material could be worked as a fluorescent probe for Fe^{3+}. Figs. S4–S7 show the absorption, PL spectra, and emission colors of DPP monomers in the presence of various cation ions. The fluorescence spectral responses of M1 and M2 solutions with Fe^{3+} were also evaluated (Fig. S8). Both M1 and M2 showed sensitivity toward Fe^{3+}, with the K_{sv} of 9.05×10^2 and 4.07×10^2 M^{-1}, respectively. The detection limit for M1 and M2 toward Fe^{3+} was 5.81×10^{-5} and 2.06×10^{-4} M, respectively. Compared with DPP monomers, PFDPP polymer exhibited enhanced sensing ability that resulted from efficient chelation between the specific fluorene-linked DPP units with Fe^{3+}. Fig. 6 shows the specificity of PFDPP toward various cations and Fe^{3+} ions. We examined other cations that could have interference with the recognition of Fe^{3+}, in which PFDPP was treated 1.0×10^{-5} M of Fe^{3+} and 1.0×10^{-5} M of other cations. The changes of the fluorescence intensity (*i.e.*, I_0/I) of PFDPP were studied and measured on the addition of different cations. Only Fe^{2+} has a slight effect on the recognition of Fe^{3+}, as shown in the black bars in Fig. 6. Then, adding 1×10^{-5} M of Fe^{3+} in PFDPP solutions could yield 35- to 200-fold emission increase with and without other metal ions, respectively (Fig. 6, red bar). As a result, the presence of other metal ions did not have affected the response of PFDPP toward Fe^{3+}, except for the anticipated quenching effect from Fe^{2+}.

3.5. *Anion sensing properties*

Fig. 7 shows the PL spectra, PL response profiles, and fluorescence emissions colors of PFDPP in the presence of F^-, Cl^-, Br^-, I^-, NO_2^-, NO_3^-, HSO_4^-, CN^-, SCN^-, and PO_4^{3-}. As presented in Fig. 7(a) and (b), the PFDPP in THF solution emitted yellow color, and its fluorescence peaks centered at 550 and 590 nm. We found that after adding Cl^-, Br^-, I^-, NO_2^-, and NO_3^- into PFDPP solution, the fluorescence intensity decreased slightly; however, the F^- ions completely quenched the PFDPP solution and disappearance the yellow color (Fig. 7(c)). These results suggest that the F^- ion was induced as the most appropriate quencher to interrupt electronic energy transfer EET by strong deprotonated interaction on the lactam N positions of the DPP moiety. The strong H-F interaction resulted in deprotonation of DPP amide moiety in the presence of F^- ion, causing a dramatic change in color and

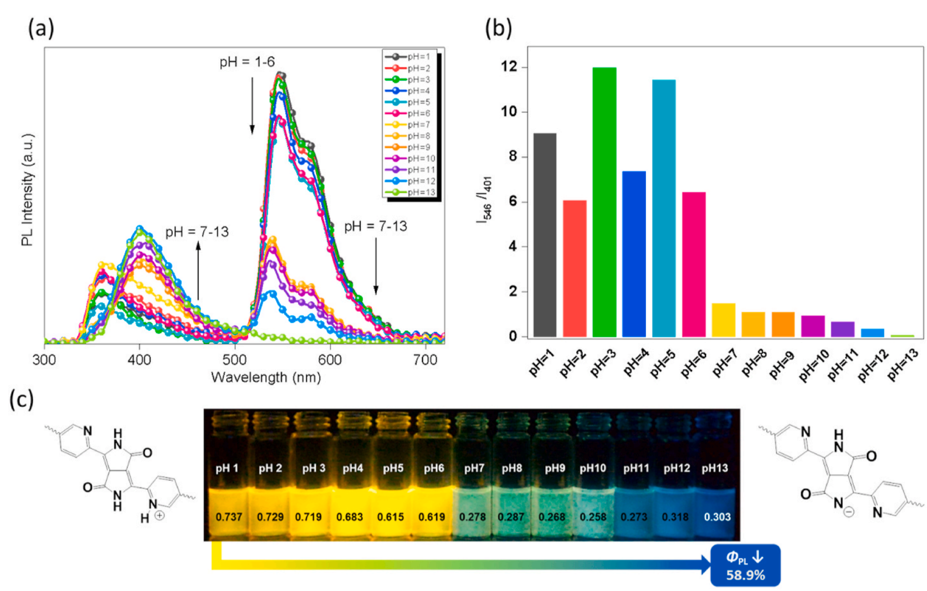

Fig. 10. (a) Photoluminescence profiles and (b) ratiometric PL response profiles of PFDPP in various pH values. The concentration of polymer: 1.0×10^{-6} M in THF. The excitation wavelength is 350 nm. (a) Fluorescence images of PFDPP solution in various pH values and (b) schematic representation of protonation and deprotonation for DPP structures. The excitation wavelength is 350 nm.

fluorescence of the compounds.

Fig. 8 represents the absorption and photoluminescence titration measurements of PFDPP using different concentrations of F^- from 0 to 136 μM. As observed when the concentration of F^- was zero, PFDPP had two absorption peaks at 490 and 520 nm, and their absorption intensities were gradually decreased when the concentration of F^- anion increased due to the deprotonation process of DDP units with fluoride ions (Fig. 8(a)). In addition, the emission intensities of PFDPP at 547 nm gradually decreased with increasing concentration of F^- anion and were completely quenched when the concentration of F^- was 136 μM ((Fig. 8 (b)).

Fig. 9 shows the specificity of PFDPP toward F^- ions in the presence of other various metal anions. The results showed that there is partial fluorescence quenching of PFDPP in the presence of CN^- ions, and no effect for PFDPP response toward F^- in the presence of other metal anions. For comparison, Table S1 collects the literature concerning DPP-functionalized chromophores prepared from PD and different precursors [49,51–58]. As observed from Table S1, this study offers an effective sensing performance (i.e., cation and anion) as compared to other conjugated polymers or low molecular weight chromophores.

Fig. 10 showed the fluorescence properties of PFDPP at various pH from 1 to 13. The PL curve of PFDPP in THF solution does not show any big changes in the maximum emission peak of PFDPP when the increasing the solution acidity from 6 to 1 and their color was yellow due to the protonation of pyridine moiety in the PFDPP polymer backbone (Fig. 10(a)–(c)). While, when the pH values increase from 7 to 10, there is dramatically changed in the FL properties of PFDPP, and color solutions changes from yellow to pale green (Fig. 10(c)). Finally, when the pH values increase from 10 to 13 and increasing the basicity of PFDPP solution, the emission intensity of PFDPP was decreased and completely quenched at pH = 13 and a new FL peak appeared at 410 nm. Furthermore, at pH = 13, the PFDPP solution emits blue color (Fig. 10 (c)), which is attributed to the deprotonation of DDP lactam N groups.

4. Conclusions

To conclude, in this work, we synthesized a new conjugated polymer PFDPP containing diketopyrrolopyrrole through Suzuki coupling polymerization. The chemical structure and M_w of PFDPP were determined by NMR and GPC analyses. According to the absorbance and photoluminescence experiments of PFDPP toward different kinds of cations and anions, the results indicated that the PFDPP material showed excellent sensitivity for Fe^{3+} and F^- ions with the Stern-Volmer constants of 2.3×10^5 M^{-1} and 1.05×10^5 M^{-1}, respectively, and the limit of detection values of PFDPP were 1.31×10^{-6} and 1.81×10^{-6} M for Fe^{3+} and F^-; respectively. Furthermore, the PFDPP polymer displayed changes in color emission when increasing the basicity of the solution by using NaOH solution. We believe that the PFDPP precursor could be used as an emerging candidate for chemosensory and environmental applications.

CRediT authorship contribution statement

Mohamed Gamal Mohamed: Methodology, Conceptualization, Data curation, Investigation, Writing – original draft. **Yu-Shan Chou:** Methodology, Conceptualization, Data curation, Investigation. **Po-Chih Yang:** Conceptualization, Methodology, Data curation, Supervision, Writing – review & editing. **Shiao-Wei Kuo:** Conceptualization, Methodology, Data curation, Supervision, Writing – review & editing.

Declaration of competing interest

The authors declare that they have no known competing financial interests or personal relationships that could have appeared to influence the work reported in this paper.

Acknowledgment

Financial support for this work by grants from the Ministry of Science and Technology, Taiwan (Nos. 109-2221-E-155-053, 110-2221-E-155-001) is gratefully appreciated.

Appendix A. Supplementary data

Supplementary data to this article can be found online at https://doi.org/10.1016/j.polymer.2021.124266.

References

[1] T. Wang, N. Zhang, W. Bai, Y. Bao, Fluorescent chemosensors based on conjugated polymers with N-heterocyclic moieties: two decades of progress, Polym. Chem. 11 (2020) 3095–3114.
[2] Y. Yang, G. Zhang, H. Luo, J. Yao, Z. Liu, D. Zhang, Highly sensitive thin-film field-effect transistor sensor for ammonia with the DPP-Bithiophene conjugated polymer entailing thermally cleavable tert-Butoxy groups in the side chains, ACS Appl. Mater. Interfaces 8 (2016) 3635–3643.
[3] M.G. Mohamed, M.Y. Tsai, C.F. Wang, C.F. Huang, M. Danko, L. Dai, T. Chen, S. W. Kuo, Multifunctional polyhedral oligomeric silsesquioxane (POSS) based hybrid porous materials for CO_2 uptake and iodine adsorption, Polymers 13 (2021) 221.
[4] M.T. Nguyen, R.A. Jones, B.J. Holliday, Recent advances in the functional applications of conducting Metallopolymers, Coord. Chem. Rev. 377 (2018) 237–258.
[5] H.R. Abuzeid, A.F.M. El-Mahdy, S.W. Kuo, Covalent organic frameworks: design principles, synthetic strategies, and diverse applications, Giant 6 (2021) 100054.
[6] M.G. Mohamed, N.Y. Liu, A.F.M. EL-Mahdy, S.W. Kuo, Ultrastable luminescent hybrid microporous polymers based on polyhedral oligomeric silsesquioxane for CO_2 uptake and metal ion sensing, Microporous Mesoporous Mater. 311 (2021) 110695.
[7] K.I. Aly, M.M. Sayed, M.G. Mohamed, S.W. Kuo, O. Younis, A facile synthetic route and dual function of network luminescent porous polyester and copolyester containing porphyrin moiety for metal ions sensor and dyes adsorption, Microporous Mesoporous Mater. 298 (2020) 110063.
[8] H.N. Kim, Z. Guo, W. Zhu, J. Yoon, H. Tian, Recent progress on polymer-based fluorescent and colorimetric chemosensors, Chem. Soc. Rev. 40 (2011) 79–93.
[9] L.J. Fan, Y. Zhang, C.B. Murphy, S.E. Angell, M.F.L. Parker, B.R. Flynn, W.E. Jones, Fluorescent conjugated polymer molecular wire chemosensors for transition metal ion recognition and signaling, Coord. Chem. Rev. 253 (2009) 410–422.
[10] M.G. Mohamed, T.C. Chen, S.W. Kuo, Solid-state chemical transformations to enhance gas capture in Benzoxazine-linked conjugated microporous polymers, Macromolecules 54 (2021) 5866–5877.
[11] M.G. Mohamed, S.W. Kuo, Crown Ether-functionalized polybenzoxazine for metal ion adsorption, Macromolecules 53 (2020) 2420–2429.
[12] M.G. Mohamed, E.C.A. Jr, B.M. Matsagar, J. Na, Y. Yamauchi, K.C.W. Wu, S. W. Kuo, Construction hierarchically Mesoporous/microporous materials based on block copolymer and covalent organic framework, J. Taiwan Inst. Chem. Eng. 112 (2020) 180–192.
[13] S.W. Thomas, G.D. Joly, T.M. Swager, Chemical sensors based on amplifying fluorescent conjugated polymers, Chem. Rev. 107 (2007) 1339–1386.
[14] M.G. Mohamed, M.H. Elsayed, A.M. Elewa, A.F.M. EL-Mahdy, C.H. Yang, A.A. K. Mohammed, H.H. Chou, S.W. Kuo, Pyrene-containing conjugated organic microporous polymers for photocatalytic hydrogen evolution from water, Catal. Sci. Technol. 11 (2021) 2229–2241.
[15] P.C. Yang, H. Wu, C.L. Lee, W.C. Chen, H.J. He, M.T. Chen, Triphenylamine-based linear conjugated polyfluorenes with various pendant groups: synthesis, characterization, and ion responsive properties, Polymer 54 (2013) 1080–1090.
[16] P. Bhaumick, A. Jana, L.H. Choudhury, Synthesis of novel coumarin containing conjugated fluorescent polymers by Suzuki cross-coupling reactions and their chemosensing studies for iron and mercury ions, Polymer 218 (2021) 123415.
[17] H. Zhang, K. Yang, C. Chen, Y. Wang, Z. Zhang, L. Tang, Q. Sun, S. Xue, W. Yang, 1,4-Diketo-pyrrolo[3,4-c]pyrroles (DPPs) based insoluble polymer films with lactam hydrogens as renewable fluoride anion chemosensor, Polymer 149 (2018) 266–272.
[18] A.F.M. EL-Mahdy, A.M. Elewa, S.W. Huang, H.H. Chou, S.W. Kuo, Dual-Function fluorescent covalent organic frameworks: HCl sensing and photocatalytic H_2 evolution from water, Adv. Optical Mater. 8 (2020) 2000641.
[19] L.H. Xie, C.R. Yin, W.Y. Lai, Q.L. Fan, W. Huang, Polyfluorene-based semiconductors combined with various periodic table elements for organic electronics, Prog. Polym. Sci. 37 (2012) 1192–1264.
[20] M. Knaapila, A.P. Monkman, Methods for controlling structure and photophysical properties in polyfluorene solutions and gels, Adv. Mater. 25 (2013) 1090–1108.
[21] Q. Zhao, S.H. Liu, W. Huang, Polyfluorene-based blue-emitting materials, Macromol. Chem. Phys. 210 (2009) 1580–1590.
[22] P.B. Balanda, M.B. Ramey, J.R. Reynolds, Water-soluble and blue luminescent cationic polyelectrolytes based on poly(p-phenylene), Macromolecules 32 (1999) 3970–3978.
[23] G. Zhou, Y. Cheng, L. Wang, F. Wang, Novel polyphenylenes containing phenol-substituted oxadiazole moieties as fluorescent chemosensors for fluoride ion, Macromolecules 28 (2005) 2148–2153.

[24] K.I. Aly, O. Younis, M.H. Mahross, E.A. Orabi, M.A. Hakim, O. Tsutsumi, M. G. Mohamed, M.M. Sayed, Conducting copolymers nanocomposite coatings with aggregation-controlled luminescence and efficient corrosion inhibition properties, Prog. Org. Coat. 135 (2019) 525–535.

[25] S. Qu, W. Wu, J. Hua, C. Kong, Y. Long, H. Tian, New diketopyrrolopyrrole(DPP) dyes for efficient dye-sensitized solar cells, J. Phys. Chem. C 114 (2010) 1343–1349.

[26] W.J. Xiao, Y. Wang, W.R. Wang, J. Li, J. Wang, Z.W. Xu, J. Li, J. Yao, W.S. Li, Diketopyrrolopyrrole-based Donor−Acceptor conjugated microporous polymers for visible-light-driven photocatalytic hydrogen production from water, Macromolecules 53 (2020) 2454–2463.

[27] S.I. Lim, J. Koo, J. Jang, M. Oh, D.T. Tran, S. Park, Y. Cao, D.Y. Kim, K.U. Jeong, Development of diketopyrrolopyrrole-based smart inks by substituting ionic pendants and engineering molecular packing structures, ACS Appl. Mater. Interfaces 13 (2021) 31206–31214.

[28] A.D. Hendsbee, J.P. Sun, L.R. Rutledge, I.G. Hill, G.C. Welch, Electron deficient diketopyrrolopyrrole dyes for organic electronics: synthesis by direct arylation, optoelectronic characterization, and charge carrier mobility, J. Mater. Chem. A 2 (2014) 4198–4207.

[29] E.D. Głowacki, H. Coskun, M.A. Blood-Forsythe, U. Monkowius, L. Leonat, M. Grzybowski, D. Gryko, M.S. White, A. Aspuru-Guzik, N.S. Sariciftci, Hydrogen-bonded diketopyrrolopyrrole (DPP) pigments as organic semiconductors, Org. Electron. 15 (2014) 3521–3528.

[30] Y. Zhu, A.R. Rabindranath, T. Beyerlein, B. Tieke, Highly luminescent 1,4-diketo-3,6-diphenylpyrrolo[3,4-c]pyrrole-(DPP-) based conjugated polymers prepared upon Suzuki coupling, Macromolecules 40 (2007) 6981–6989.

[31] T. He, Y. Gao, S. Sreejith, X. Tian, L. Liu, Y. Wang, H. Joshi, S.Z.F. Phua, S. Yao, X. Lin, Y. Zhao, A.C. Grimsdale, H. Sun, Biocompatible two-photon absorbing dipyridyldiketopyrrolopyrroles for metal-ion-mediated self-assembly modulation and fluorescence imaging, Adv. Opt. Mater. 4 (2016) 746–755.

[32] H. Ftouni, F. Bolze, H. de Rocquigny, J.-F. Nicoud, Functionalized two-photon absorbing diketopyrrolopyrrole-based fluorophores for living cells fluorescent microscopy, Bioconjug. Chem. 24 (2013) 942–950.

[33] J. Schmitt, V. Heitz, A. Sour, F. Bolze, H. Ftouni, J.-F. Nicoud, L. Flamigni, B. Ventura, Diketopyrrolopyrrole-porphyrin conjugates with high two-photon absorption and singlet oxygen generation for two-photon photodynamic therapy, Angew. Chem. 54 (2015) 169–173.

[34] Y. Gao, G. Feng, T. Jiang, C. Goh, L. Ng, B. Liu, B. Li, L. Yang, J. Hua, H. Tian, Biocompatible nanoparticles based on diketo-pyrrolo-pyrrole (DPP) with aggregation-induced red/NIR emission for in vivo two-photon fluorescence imaging, Adv. Funct. Mater. 25 (2015) 2857–2866.

[35] K. Nie, S. Xu, X. Duan, H. Shi, B. Dong, M. Long, H. Xu, X.F. Jiang, Z. Liu, Diketopyrrolopyrrole-doped hybrid FONs as two-photon absorbing and dual-emission fluorescent nanosensors for Hg^{2+}, Sens. Actuators B Chem. 265 (2018) 1–9.

[36] M. Grzybowski, D.T. Gryko, Diketopyrrolopyrroles: synthesis, reactivity, and optical properties, Adv. Optical Mater. 3 (2015) 280–320.

[37] Q. Niu, X. Wu, T. Li, Y. Cui, S. Zhang, X. Li, Highly selective, sensitive and fast-responsive fluorescent sensor for Hg(2, Spectrochim. Acta A Mol. Biomol. Spectrosc. 163 (2016) 45–48.

[38] X.D. Jiang, J. Zhao, Q. Li, C.L. Sun, J. Guan, G.T. Sun, Synthesis of NIR fluorescent thienyl-containing aza-BODIPY and its application for detection of Hg^{2+} Electron transfer by bonding with Hg^{2+}, Dyes Pigm 125 (2016) 136–141.

[39] Y. Jiao, L. Zhang, P. Zhou, A rhodamine B-based fluorescent sensor toward highly selective mercury (II) ions detection, Talanta 150 (2016) 14–19.

[40] Y. Jiang, Y. Wang, J. Hua, S. Qu, S. Qian, H. Tian, Synthesis and two-photon absorption properties of hyperbranched diketo-pyrrolo-pyrrole polymer with triphenylamine as the core, J. Polym. Sci. Part A 47 (2009) 4400–4408.

[41] M. Kaur, D.H. Choi, Diketopyrrolopyrrole: brilliant red pigment dye-based fluorescent probes and their applications, Chem. Soc. Rev. 44 (2015) 58–77.

[42] X. Zou, S. Cui, J. Li, X. Wei, M. Zheng, Diketopyrrolopyrrole based organic semiconductor materials for field-effect transistors, Front Chem 9 (2021) 671294.

[43] J.E. Donaghey, E.H. Sohn, R.S. Ashraf, T.D. Anthopoulos, S.E. Watkins, K. Song, C. K. Williams, I. McCulloch, Pyrroloindacenodithiophene polymers: the effect of molecular structure on OFET performance, Polym. Chem. 4 (2013) 3537–3544.

[44] D. Chandran, T. Marszalek, W. Zajaczkowski, P.K. Madathil, R.K. Vijayaraghavan, Y.-H. Koh, S.Y. Park, J.R. Ochsmann, W. Pisula, K.S. Lee, Thin film morphology and charge mobility of diketopyrrolopyrrole based conjugated polymers, Polymer 73 (2015) 205–213.

[45] X. Wang, Y. Wen, H. Luo, G. Yu, X. Li, Y. Liu, H. Wang, Donor-acceptor copolymer based on dioctylporphyrin: synthesis and application in organic field-effect transistors, Polymer 53 (2012) 1864–1869.

[46] H. Zhang, K. Yang, K. Zhang, Z. Zhang, Q. Sun, W. Yang, Thionating iso-diketopyrrolopyrrole-based polymers: from p-type to ambipolar field effect transistors with enhanced charge mobility, Polym. Chem. 9 (2018) 1807–1814.

[47] Y. Qu, J. Hua, H. Tian, Colorimetric and ratiometric red fluorescent chemosensor for fluoride ion based on diketopyrrolopyrrole, Org. Lett. 12 (2010) 3320–3323.

[48] Z. Liu, K. Zhang, Q. Sun, Z. Zhang, L. Tang, S. Xue, D. Chen, H. Zhang, W. Yang, Synthesis and remarkable mechano- and thermos-hypsochromic luminescence of a new type of DPP-based derivative, J. Mater. Chem. C 6 (2018) 1377–1383.

[49] Y. Qu, S. Qu, L. Yang, J. Hua, D. Qu, A red-emission diketopyrrolopyrrole-based fluoride ion chemosensor with high contrast ratio working in a dual mode: solvent-dependent ratiometric and "turn on" pathways, Sens. Actuators B Chem. 173 (2012) 225–233.

[50] D. Cao, Q. Liu, W. Zeng, S. Han, J. Peng, S. Liu, Synthesis and characterization of novel red-emitting alternating copolymers based on fluorene and diketopyrrolopyrrole derivatives, J. Polym. Sci. Part A 44 (2006) 2395–2405.

[51] L. Wang, L. Yang, L. Huang, D. Cao, Diketopyrrolopyrrole-derived Schiff base as colorimetric and fluoromertic probe for sequential detection of HSO_4^- and Fe^{3+} with "off-on-off" response, Sens. Actuators B Chem. 209 (2015) 536–544.

[52] M. Kaur, D.H. Choi, Dual channel receptor based on diketopyrrolopyrrole alkyne conjugate for detection of Hg^{2+}/Cu^{2+} by "naked eye" and fluorescence, Sens. Actuators B Chem. 190 (2014) 542–548.

[53] A.O. Weldeab, L. Li, S. Cekli, K.A. Abboud, K.S. Schanze, R.K. Castellano, Pyridine-terminated low gap π-conjugated oligomers: design, synthesis, and photophysical response to protonation and metalation, Org. Chem. Front. 5 (2018) 3170–3177.

[54] M.V.R. Raju, H.C. Lin, A novel diketopyrrolopyrrole (DPP)-based [2]rotaxane for highly selective optical sensing of fluoride, Org. Lett. 15 (2013) 1274–1277.

[55] Y. Qu, Y. Wu, Y. Gao, S. Qu, L. Yang, J. Hua, Diketopyrrolopyrrole-based fluorescent conjugated polymer for application of sensing fluoride ion and bioimaging, Sens. Actuators B Chem. 197 (2014) 13–19.

[56] L. Deng, W. Wu, H. Guo, J. Zhao, S. Ji, X. Zhang, X. Yuan, C. Zhang, Colorimetric and ratiometric fluorescent chemosensor based on diketopyrrolopyrrole for selective detection of thiols: an experimental and theoretical study, J. Org. Chem. 76 (2011) 9294–9304.

[57] S. Lin, S. Liu, F. Ye, L. Xu, W. Zeng, L. Wang, L. Li, R. Beuerman, D. Cao, Sensitive detection of DNA by hyperbranched diketopyrrolopyrrole-based conjugated polyelectrolytes, Sens. Actuators B Chem. 182 (2013) 176–183.

[58] T.K. Ghorpade, M. Patri, S.P. Mishra, Highly sensitive colorimetric and fluorometric anion sensors based on mono and di-calix[4]pyrrole substituted diketopyrrolopyrroles, Sens. Actuators B Chem. 225 (2016) 428–435.